Measurement of the left-right asymmetry in $\pi^- p \to \gamma n$ from 301 to 625 MeV/c at backward angles

G. J. Kim*, J. Engelage,[†] B. M. K. Nefkens, and H. J. Ziock[‡]

Department of Physics, University of California at Los Angeles, Los Angeles, California 90024

J. Arends[§]

Department of Physics, University of California at Los Angeles, Los Angeles, California 90024
and Department of Physics, Catholic University of America, Washington, D.C. 20064

W. J. Briscoe

Department of Physics, The George Washington University, Washington, D.C. 20052

M. E. Sadler

Department of Physics, Abilene Christian University, Abilene, Texas 79699
(Received 4 April 1990)

The left-right asymmetry of $\pi^- p \to \gamma n$ has been measured using a transversely polarized target at seven pion momenta from 301 to 625 MeV/c, mostly at photon angles of 90° and 110° c.m. The final-state γ and neutron were detected in coincidence. Neutrons were recorded in two arrays of plastic scintillators and the γ's in two matching sets of lead-glass counters. The results are compared with the predictions from the two most recent single-pion photoproduction partial-wave analyses. The agreement with the analysis of Arai and Fujii is poor, casting some doubt on the correctness of their values for the radiative decay amplitude of the neutral Roper resonance which are used widely. The agreement is much better with the results of the VPI analysis. Also, a comparison is made with the recoil-proton polarization data from the inverse reaction measured at 90° with a deuterium target. It reveals substantial discrepancies, indicating the shortcomings of the deuterium experiments for neutron target experiments. Our data are also compared with several bag-model calculations.

I. INTRODUCTION

The radiative decays of the N^* and Δ resonances occupy a special place in the development of modern particle physics. The original second and third πN resonances, now known as $D_{13}(1520)$ and $F_{15}(1680)$, were discovered in pion photoproduction studies[1] which helped to elucidate the nature of the first resonance $\Delta(1232)$. Shortly after the introduction of quarks into particle physics, a complete hadron spectroscopy based on quarks was proposed[2] which later developed into the widely used quark bag model. The quark model gained considerable credibility with the successful calculation of the magnitude and sign of some 24 radiative transition amplitudes of low-mass πN resonances.[3,4] A flash of new excitement has been generated by the suggestion[5] that color magnetism may be investigated in pion photoproduction, namely, by a measurement of the $E2$ radiative transition of the Δ. The proposed existence of hybrid states[6,7] consisting of three quarks and a glueball may be tested in radiative decays. The lowest-lying hybrid may have a mass[8] close to that of $P_{11}(1440)$. One can test this hypothesis by ex-

amining the radiative decay of the charged and neutral modes of P_{11}.[9] The photoexcitation of the lightest hybrid baryon is strongly suppressed in the production on a proton, but allowed on a neutron, a result that resembles the quark-model selection rules of Moorhouse.[10]

Progress in pion-photoproduction phenomenology has been slow due to the complexity of the multipole analysis. Each of the four single-pion photoproduction channels is described by four complex amplitudes requiring 28 input data at each energy and angle or 28 different measurements. The need for the large number of inputs is aggravated by the shortage of monochromatic photon beams and the lack of a free neutron target. CEBAF is expected to improve dramatically the experimental possibilities for π^+ and π^0 photoproduction on protons.

We have investigated a channel that is not easily accessible at CEBAF, namely π^- photoproduction on a neutron. It is accomplished by studying the inverse process

$$\pi^- p \to \gamma n \ .$$

This reaction may be measured at LAMPF up to a total energy of 1.47 GeV thanks to good π^- beams to 650

TABLE I. Multipoles for N^* resonances in pion photoproduction.

Photon state	Multipole name	Resonance	Angular distribution
$M1$	M_{1+} mag. dipole	$P_{33}(1232)$	$2+3\sin^2\theta$
$E2$	E_{1+} elect. quad.	$P_{33}(1232)$	$1+\cos^2\theta$
$M1$	M_{1-} mag. dipole	$P_{11}(1440)$	1
$E1$	E_{0+} elect. dipole	$S_{11}(1535)$	1
$E1$	E_{2-} elect. dipole	$D_{13}(1520)$	$2+3\sin^2\theta$
$M2$	M_{2-} mag. quad.	$D_{13}(1520)$	$1+\cos^2\theta$

MeV/c. This approach solves both problems of the lack of a neutron target and a monochromatic photon beam. The price is the construction of a complex experimental setup to discriminate against the charge-exchange (CEX) background $\pi^-p \rightarrow \pi^0 n$, which has cross sections 30 to 100 times larger than those for radiative exchange (REX) $\pi^-p \rightarrow \gamma n$.

In the following we describe an experiment to measure the left-right asymmetry A_N in REX using a transversely polarized hydrogen target in the energy region of the $\Delta(1232)$ and Roper, $N^*(1440)$, resonances. Except for a measurement[11] at one energy much below the $N^*(1440)$, A_N(REX) has never been measured before. Our data by themselves are insufficient, obviously, to extract all of the physics alluded to earlier, but they are absolutely necessary for making a full $\gamma n \rightarrow \pi^-p$ multipole analysis to determine the radiative decay amplitudes of neutral πN resonances. Our left-right-asymmetry data may be compared to the recoil-proton polarization of the inverse reaction obtained using a deuterium target. Time-reversal invariance requires $A_N = P$. There was a flurry of activity in the late 1960's to test the detailed balance, which was prompted by a suggestion that time-reversal invariance may not be respected in the electromagnetic interactions of hadrons.[12] No evidence for T violation has been found and the consensus now is that detailed balance is valid to a high degree in electromagnetic interactions of hadrons such as $\pi^-p \rightarrow \gamma n$. Because the $\gamma n \rightarrow \pi^-p$ measurements that are based on $\gamma d \rightarrow \pi^-X$ experiments require extensive deuterium corrections, one can make a comparison of $\gamma n \rightarrow \pi^-p$ data with $\pi^-p \rightarrow \gamma n$ results to check the validity of these corrections. We will see later that our A_N results do not agree with published values of

P. In a separate paper,[13] we have shown that $d\sigma(\pi^-p \rightarrow \gamma n)$ does not fully equate to the inverse either. This, unfortunately, implies that radiative decay amplitudes of the neutral πN resonances, which are all derived from $\gamma d \rightarrow \pi^-X$ experiments, are likely somewhat in error.

The formalism for describing pion photoproduction is readily available in the literature. The two most used systems are based on helicity amplitudes and on electromagnetic multipoles.

The left-right asymmetry from a transversely polarized proton target in terms of the four complex helicity amplitudes, H_1 to H_4 of Walker,[14] is given by

$$A_N(\theta) = -\frac{k}{q}\frac{1}{d\sigma/d\Omega}\mathrm{Im}(H_1H_3^* + H_2H_4^*)$$

with

$$\frac{d\sigma}{d\Omega} = \frac{1}{2}\frac{k}{q}(|H_1|^2 + |H_2|^2 + |H_3|^2 + |H_4|^2),$$

where q and k are the pion and photon c.m. momenta, respectively. The expression for A_N implies that a minimum of two helicity amplitudes with different phases is needed for an asymmetry.

An alternate description of pion photoproduction may be obtained by expanding the incoming photon waves into eigenstates of the total angular momentum L of the photon called electric and magnetic multipoles, EL and ML, see Table I. To generate a left-right asymmetry, one needs at least two multipoles. At 90° in the c.m., there is a special condition; namely, the interfering multipoles must have opposite parity. At this angle the left-right asymmetry for waves up to $L=2$ is[15]

$$A_N = \frac{k}{q}\frac{1}{d\sigma/d\Omega}\mathrm{Im}[-E_{0+}(2M_{1-} + M_{1+} + 3E_{1+})^* - 6E_{1+}E_{2-}^* + M_{1-}(3M_{2-} - E_{2-})^* + M_{1+}(6M_{2-} + 4E_{2-})^*]. \quad (1)$$

This expression serves to illustrate the complexity of photoproduction analysis even at low energies.

II. EXPERIMENT

The left-right asymmetry A_N for $\pi^-p \rightarrow \gamma n$ (REX) was measured at pion momenta of 301, 316, 427, 471, 547, 586, and 625 MeV/c using a transversely polarized proton target. Instead of measuring the left and right scattering cross sections on a proton target with the spins aligned vertically, we measured the transversity up and

down cross sections referring to scattering from a polarized proton target with spin up and down, respectively. Reversing the proton spin from up to down is considerably more practical than interchanging our large detectors between beam left and beam right. The main photon angles were about 90° and 110° c.m., except at 301 and 316 MeV/c where the data were taken at 50° instead of 110°. The experiment was performed in the Pion and Particle Physics (P^3) channel at the Cinton P. Anderson Meson Physics Facility (LAMPF) of the Los Alamos National Laboratory. Some preliminary results have been
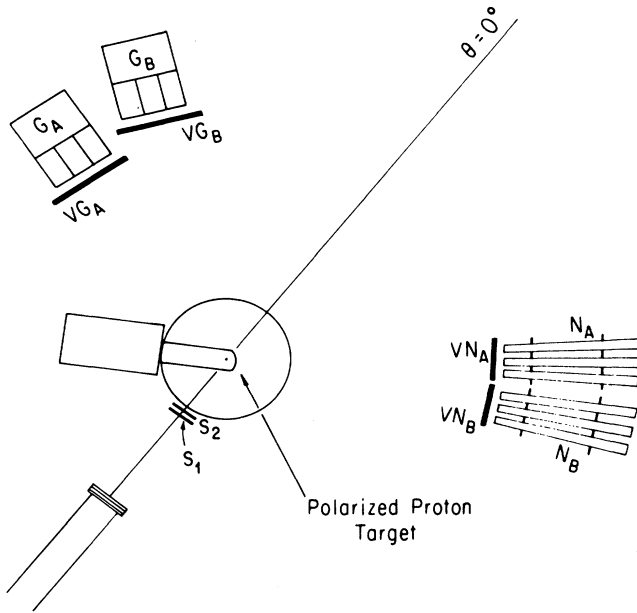
FIG. 1. Schematic of the experimental setup. S_1 and S_2 are thin beam monitoring counters. N_A and N_B are the two sets of 15 neutron counters, and G_A and G_B are the two sets of matching 15 γ counters. VN_A and VN_B, and VG_A and VG_B are charged-particle veto counters placed in front of the neutron and γ counters.

published already.[13,16]

Figure 1 shows the experimental setup. A detailed description is given elsewhere.[17,18] The setup selectively enhanced the detection of the REX events over CEX, $\pi^- p \rightarrow \pi^0 n \rightarrow 2\gamma n$, by exploiting the two-body kinematic correlation in the REX final state. The final-state γ was detected using two independent sets of 15 γ counters each, arranged in a rectangular 5 (vertical) by 3 (horizontal) configuration. The neutron was detected in coincidence in two corresponding sets of 15 neutron counters, see Fig. 2. The two independent γ-neutron matching sets provided two angle measurements simultaneously. Each of the γ counters was a 15×15-cm^2, 25-cm-deep lead-glass block viewed by a 12.7-cm photomultiplier tube. Each neutron counter consisted of a 45.7-cm-long cylindrical plastic scintillator viewed by a 5-cm photomulti-
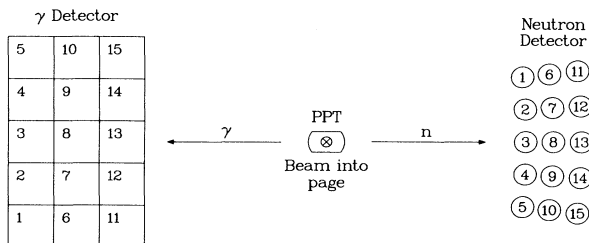
FIG. 2. Front view of neutron and γ counter arrays showing the one-to-one neutron-γ counter matching for REX.

plier tube. The neutron counters were carefully arranged to give one-to-one neutron-to-γ counter matching according to the REX kinematics. For each neutron counter the REX γ can go to one of the 15 γ counters, whereas the CEX γ's illuminate the entire front of all 15 γ counters.

The data were collected in 5 to 8 pairs of spin-up and -down polarization runs, each lasting about 4 h. The polarization was reversed every 8 h to ensure identical experimental conditions for each spin pair, and to minimize any long term drifts in the hardware. The target polarization averaged 78–81 % for all spin-up and -down runs. The polarization was monitored throughout the experiment using NMR technique.

A concise description of the pion beam, polarized proton target, γ and neutron counters, event-trigger arrangement, and data-acquisition system is given in Ref. 18.

III. DATA ANALYSIS

The major challenge of the data analysis was obtaining a clean separation between the REX and the CEX events. For most of our detector positions, the neutron time-of-flight (TOF) information was of little help in this separation process as the REX-CEX neutron TOF difference was less than 1 nsec. The γ pulse-height information was insufficient to discriminate fully between the REX and the CEX γ's because of the overlap in energy between the REX and CEX γ's and the modest energy resolution, about 25%, of the lead-glass γ counters. CEX, with a cross section 30 to 100 times larger than REX, represented a potentially dangerous polarization-dependent background to REX.

The two-body REX kinematics allowed us to impose angular correlation and coplanarity requirements between the detected γ and neutron, which were incorporated in the one-to-one neutron-to-γ counter arrangement used in the experiment. For each neutron counter, the matched γ counter yielded the bulk of the REX events along with some CEX contamination which was subtracted to give the true number of the REX events. The event sample was selected by application of a neutron TOF window, typically 3 nsec wide (see Fig. 3), and by a photon pulse-height cut, typically > 180 MeV. From this sample we subtracted the nonhydrogenic background using "dummy" target data. The event distribution of the extracted REX and CEX events over the 15 γ counters for each neutron counter clearly indicated a REX enhancement on top of a broad CEX background. Shown in Fig. 4 is the event distribution for neutron counter 10 at 625 MeV/c 90° c.m.; the spin-up and the spin-down distributions have been added to improve the statistics. The shape of the CEX event distribution was obtained using Monte Carlo calculations. The CEX contamination in the coplanar REX counter was obtained by extrapolation using the Monte Carlo–generated CEX distribution normalized to fit the noncoplanar and nonadjacent data; in Fig. 4, the matched γ counter 10 and the adjacent counters 5, 9, and 15 were not used in this fitting. As one can see from the figure, there is good agreement between the experiment and the Monte
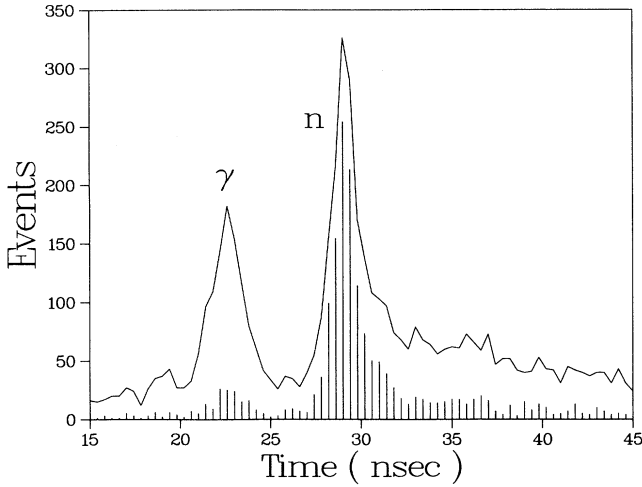
FIG. 3. Typical time of flight for one of the neutron counters. The contour plot is the raw data, and the bar plot shows the spectrum after applying the pulse-height cut on the γ signals.

Carlo–generated CEX event distribution. We deduce from the figure that out of 275 events in the matched counter, about 185 events are REX events, the rest are CEX.

The REX asymmetry was calculated using a modified version of the general expression for the left-right asymmetry,

$$A_N = (1/P_t)(N_\uparrow - N_\downarrow)/(N_\uparrow + N_\downarrow - 2B) ,$$

where P_t is the target polarization, $N_\uparrow$ is the yield of good events from the spin-up target, $N_\downarrow$ is the normalized yield from the spin-down target, and B is the nor-
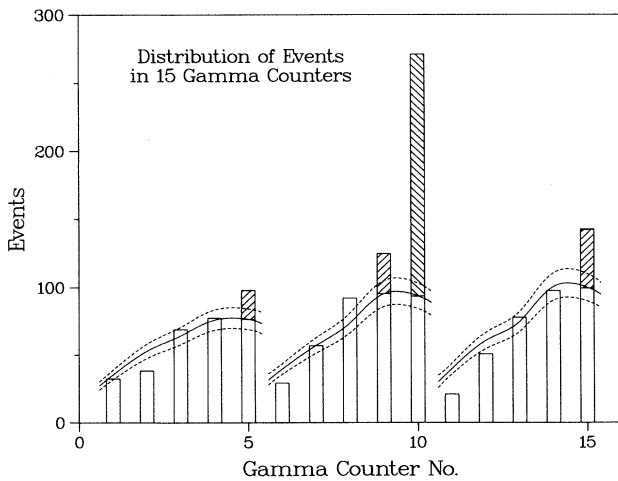
FIG. 4. Event distribution in the γ counters for neutron counter No. 10 at 625 MeV/c, 90°. The solid curve is the Monte Carlo–generated CEX distribution normalized to fit the CEX data, and the dashed curves represent a ±10% uncertainty in the normalization.

malized background yield. The complete expression explicitly includes the subtraction of the CEX contamination in the coplanar neutron-γ counter using the Monte Carlo–generated CEX event distribution. The REX asymmetry observed in neutron counter i is given by

$$A_N^{\text{REX}}(i) = \frac{1}{P_t} \frac{N_\uparrow^{\text{REX}}(i) - N_\downarrow^{\text{REX}}(i)}{N_\uparrow^{\text{REX}}(i) + N_\downarrow^{\text{REX}}(i)} ,$$

where

$$N_\uparrow^{\text{REX}}(i) = N_{\uparrow ii} - B_{ii} - \frac{1}{J} \sum_j f_{ij}(N_{\uparrow ij} - B_{ij})$$

and

$$N_\downarrow^{\text{REX}}(i) = N_{\downarrow ii} - B_{ii} - \frac{1}{J} \sum_j f_{ij}(N_{\downarrow ij} - B_{ij}) .$$

$N_{\uparrow ij}$, $N_{\downarrow ij}$, and B_{ij} denote the number of spin-up, spin-down, and background events, respectively, detected in neutron counter i in coincidence with γ counter j. The number of REX events was obtained by subtracting from the number of the REX candidate events in the matched coplanar counter N_{ii}, the nonhydrogenic background B_{ii}, and the CEX contamination as given by the sum term in the equation. The number of CEX events in the matched γ counter was evaluated using the average of the number of CEX events in the noncoplanar and nonadjacent counters, $(N_{ij} - B_{ij})$, multiplied by the Monte Carlo CEX event distribution factor f_{ij}, which relates the number of CEX events expected in γ counter j to the matched γ counter i.

For every data set, the REX asymmetry values were calculated three times using three different neutron TOF cuts. The results for the 12 data points at 625 MeV/c are shown in Table II, where three REX asymmetry values were calculated for TOF cut A, B, and C. The TOF cut A is the biggest with a width of 2.5 nsec, cut B is slightly narrower at 2.0 nsec, and cut C is the narrowest with 1.5 nsec. The narrow TOF cut removes some fraction of the CEX events, but retains most of the REX events, thus improving the REX-to-CEX event ratio. The average REX-to-CEX event ratio at 625 MeV/c with the TOF cut A is 2.2 and the ratio improves to 3.5 for the TOF cut C. Although the cut C has the best REX-to-CEX event ratio, usually the compromise cut B is preferred, because it has fewer background CEX events than cut A, and cut C suffers from poorer CEX normalization because there are not enough CEX events outside the REX kinematic region. As one can see from the table, the asymmetry values are very consistent for different TOF cuts.

The greatest difficulty in obtaining the REX asymmetry is the reliable subtraction of the CEX contamination from the good events to yield the true number of REX events. The CEX events represent a large polarization-dependent background, especially dangerous at those points where the REX and the CEX asymmetries differ in sign. The reliability of the CEX subtraction and the errors on the REX asymmetry values were examined by varying the number of CEX events by ±10%. Recall that the number of CEX events in the matched counter

TABLE II. 625-MeV/c REX asymmetry values for three different neutron TOF cuts.

$\tilde{\theta}\gamma$ (deg)	Cut A A_N	σ_{A_N}	Cut B A_N	σ_{A_N}	Cut C A_N	σ_{A_N}	REX$_\uparrow$	CEX$_\uparrow$	Events in cut B Bkgrd	REX$_\downarrow$	CEX$_\downarrow$
71.4	−0.23	0.06	−0.21	0.06	−0.22	0.06	387	617	63	574	59
74.8	−0.11	0.07	−0.13	0.07	−0.14	0.06	366	548	74	470	64
78.1	−0.14	0.06	−0.17	0.06	−0.17	0.06	379	438	55	495	52
86.4	−0.12	0.06	−0.14	0.05	−0.20	0.05	432	412	44	547	97
90.0	−0.19	0.06	−0.17	0.06	−0.19	0.05	379	327	28	502	101
93.6	−0.27	0.06	−0.21	0.06	−0.23	0.05	362	276	52	512	102
101.2	−0.16	0.06	−0.19	0.06	−0.21	0.06	354	232	49	484	128
105.0	−0.26	0.06	−0.25	0.06	−0.24	0.06	268	149	42	408	89
108.7	−0.14	0.06	−0.14	0.06	−0.16	0.06	336	155	33	420	92
116.5	−0.22	0.07	−0.20	0.06	−0.21	0.07	233	100	21	324	60
120.0	−0.22	0.07	−0.23	0.07	−0.19	0.07	175	65	8	255	28
123.3	−0.20	0.07	−0.21	0.07	−0.19	0.07	204	72	21	289	28

was determined by normalizing the Monte Carlo–generated CEX event distribution to the noncoplanar and the nonadjacent data. The normalization factor used in fitting the Monte Carlo–CEX event distribution to the experimental data was precisely the mean of the ratios of the experimental numbers of events with respect to the Monte Carlo numbers of events found in the noncoplanar and nonadjacent counters. The standard deviation in the mean ranged from 5 to 25 %. The large 15 to 25% errors occurred mostly for the 90° spin-down data where because of the large CEX asymmetries the fitting suffered from the lack of statistics. When the two spin directions were added, the uncertainty was 4 to 10 %. A ±10% variation in the CEX normalization is shown in Fig. 4. The effect on the REX asymmetry values due to one σ variation in the CEX normalization is demonstrated in Table III. The variation in the asymmetries is small compared to the calculated statistical errors. For the final REX asymmetry values, the errors due the uncertainty in the CEX normalizations, in both the spin-up and -down fittings, have been added in quadrature.

The REX asymmetries were affected very little by the uncertainty in the normalization of the nonhydrogenic background because of the very small number of background events remaining after the application of neutron TOF and γ pulse-height cuts.

IV. RESULTS AND DISCUSSION

The results for the left-right-asymmetry parameter A_N in $\pi^- p \rightarrow \gamma n$ at 301, 316, 427, 471, 547, 586, and 625 MeV/c are listed in Table IV. The errors given in the table represent the statistical and the CEX background normalization errors. The 4% systematic uncertainty in the absolute calibration of the target polarization is not included.

The results listed in Table IV are plotted in Figs. 5(a)–5(g) together with the predictions from recent energy-dependent partial-wave analyses (PWA's) of single-pion photoproduction. In Fig. 5(c), a comparison is made with the only other measurement of the REX asymmetry, a few points at 427 MeV/c by Alder et al.[11] The agreement with our results is good. These REX results were obtained in connection with a CEX A_N measurement, and the results are given in a figure only.

Single-pion photoproduction reactions require $4 \times 4 = 16$ complex amplitudes to describe the four isospin

TABLE III. 625-MeV/c REX asymmetry values showing the effect of varying the number of background CEX events by one standard deviation in the CEX normalization.

$\tilde{\theta}\gamma$ (deg)	×(1−σ) A_N	σ_{A_N}	Best fit A_N	σ_{A_N}	×(1+σ) A_N	σ_{A_N}
71.4	−0.19	0.06	−0.21	0.06	−0.23	0.06
74.8	−0.11	0.06	−0.13	0.07	−0.15	0.07
78.1	−0.15	0.06	−0.17	0.06	−0.19	0.06
86.4	−0.13	0.05	−0.14	0.05	−0.16	0.06
90.0	−0.16	0.05	−0.17	0.06	−0.19	0.06
93.6	−0.21	0.05	−0.21	0.06	−0.22	0.06
101.2	−0.18	0.05	−0.19	0.06	−0.21	0.06
105.0	−0.24	0.06	−0.25	0.06	−0.26	0.06
108.7	−0.13	0.05	−0.14	0.06	−0.15	0.06
116.5	−0.20	0.06	−0.20	0.06	−0.21	0.07
120.0	−0.22	0.07	−0.23	0.07	−0.24	0.07
123.3	−0.20	0.07	−0.21	0.07	−0.22	0.07

TABLE IV. Results for the left-right-asymmetry parameter A_N in $\pi^- p \to \gamma n$ measured with a transversely polarized target.

p_π (MeV/c)	$\tilde\theta_\gamma$ (deg)	$\cos\tilde\theta_\gamma$	A_N	σ_{A_N}	p_π (MeV/c)	$\tilde\theta_\gamma$ (deg)	$\cos\tilde\theta_\gamma$	A_N	σ_{A_N}
301	51.9	0.62	0.59	0.11	316	44.9	0.71	0.51	0.09
	88.0	0.04	0.62	0.10		49.8	0.65	0.56	0.11
	91.6	−0.03	0.62	0.12		85.9	0.07	0.74	0.08
	95.2	−0.09	0.54	0.17		89.5	0.01	0.71	0.09
						93.1	−0.05	0.68	0.07
427	86.5	0.06	0.44	0.06	471	86.2	0.07	0.41	0.08
	90.2	0.00	0.48	0.06		89.9	0.00	0.40	0.07
	93.8	−0.07	0.48	0.06		93.6	−0.06	0.32	0.07
	106.1	−0.28	0.55	0.07		106.3	−0.28	0.25	0.07
	109.9	−0.34	0.43	0.08		110.0	−0.34	0.46	0.09
	113.4	−0.40	0.48	0.08		113.6	−0.40	0.43	0.08
547	86.2	0.07	0.08	0.08	586	86.4	0.06	−0.04	0.08
	90.0	0.00	0.03	0.08		90.0	0.00	0.00	0.08
	93.7	−0.06	0.04	0.07		93.5	−0.06	0.00	0.08
	106.2	−0.28	0.14	0.07		106.2	−0.28	0.00	0.08
	109.9	−0.34	0.21	0.08		110.0	−0.34	−0.04	0.08
	113.5	−0.40	0.01	0.08		113.6	−0.40	−0.03	0.08
625	71.4	0.32	−0.21	0.08	625	101.2	−0.19	−0.19	0.06
	74.8	0.26	−0.13	0.08		105.0	−0.26	−0.25	0.06
	78.1	0.21	−0.17	0.08		108.7	−0.32	−0.14	0.06
	86.4	0.06	−0.14	0.07		116.5	−0.45	−0.20	0.07
	90.0	0.00	−0.17	0.07		120.0	−0.50	−0.23	0.07
	93.6	−0.06	−0.21	0.06		123.3	−0.55	−0.21	0.07

channels as compared to only 4 amplitudes for the πN system. It may not come as a surprise therefore that the pion photoproduction PWA has not reached the same refinement as the pion-nucleon PWA's. Recently, Arndt *et al.*, have extended the VPI PWA series to include pion photoproduction.[19] The details of the methods employed are not yet in print. A comparison of our results with the VPI predictions as extracted from the SAID program[20] is shown in Figs. 5(c)–5(g). The agreement is quite good. It should be mentioned that the VPI data base does not include our preliminary A_N results.[16]

The other major pion photoproduction analysis that we compare our data to is the Tokyo analysis by Arai and Fujii.[21] They used fixed-t dispersion relations, a K-matrix formalism, and a Regge-type parametrization of the invariant amplitudes in the higher-energy region. They analyzed $\gamma p \to \pi^+ n$, $\gamma p \to \pi^0 p$, and $\gamma n \to \pi^- p$ as there are basically no data on $\gamma n \to \pi^0 n$. Their predictions for the left-right asymmetry in $\pi^- p \to \gamma n$ are compared to our data in Figs. 5(a)–5(g). In general there is quite a difference, in particular at higher momenta in the 90° excitation function as shown in Fig. 6.

The older Glasgow energy-dependent analysis[22] of single-pion photoproduction has been updated by Crawford and Morton.[23] The asymmetry values are not available for comparison with our data.

The earliest of the modern PWA's to be considered is the Bonn analysis by Noelle.[24] He employed a hybrid analysis with fixed t-dispersion relations in a coupled-channel isobar calculation. His predictions are compared to our data in Figs. 5(d) and 5(f). The agreement is very good.

A good way to compare the different PWA's is by the

values of the resonance parameter for the neutral N^* resonances. For this experiment the most important resonances are the $\Delta(1232)$ and $P_{11}(1440)$ and to a lesser extent the $S_{11}(1535)$ and $D_{13}(1520)$ of which we only cover the low-energy tails. Table V lists the radiative helicity amplitudes for the first two resonances from the recent PWA's and the Particle Data Group[21] average. It is interesting to compare with a few calculations from quark models, even though no definitive conclusions about the models should be drawn from the comparison of the helicity amplitudes. This is especially true given the quality and quantity of the data points currently available on the neutral resonances. Quark models have made a steady progress. First came the nonrelativistic harmonic-oscillator potential model[29,3] and the relativistic calculations by Feynman, Kislinger, and Ravndal.[4] They were followed by the successful hyperfine interaction model of Isgur, Karl, and Koniuk,[30] and recently by the cloudy and chiral bag models.[31−38]

Substantial effort has gone into detailed model calculations. Recently, the bag models have outdone all others in popularity, particularly in calculating the properties of $\Delta(1232)$. The original MIT bag model does not obey chiral symmetry. It is therefore not expected to fare well in pion photoproduction, but the original calculations by Donoghue *et al.*[31] were not completely discouraging, see Table V, where we have listed the $M1$ transition amplitude on the proton for the $\Delta(1232)$. Improvements have come with the use of chiral bag models. Seminal calculations of pion photoproduction in the Δ region based on a cloudy bag model have been made by Kalbermann and Eisenberg[32] with considerable success, see Table V, and by Araki and Kamal,[33] who calculated pion production

on a proton target though with somewhat less numerical success. Recent versions of chiral bag models are by Weyrauch,[34] who reports excellent agreement for the M_{1+} amplitude. Furthermore, we have the work of Bermuth et al.,[35] who included $P_{11}(1440)$, and of Araki and Afnan,[36] who developed a multichannel unitarity model but have no numerical results available yet. The most recent works by Kamal and Araki[37] and Nozawa, Blankleider, and Lee[38] are compared directly with our asymmetry measurements in Figs. 5(b)–5(e) and 5(g). The predictions of Nozawa, Blankleider, and Lee are in acceptable agreement with our results at 316 MeV/c, but at 427 and 471 MeV/c they predict larger asymmetry values than ours. The agreement with the Kamal-Araki results

at 427 and 471 MeV/c is good, but again the agreement deteriorates at higher energies presumably because of the contributions from the higher-mass resonances which were not included in the model.

Yang[39] has developed a transition potential in a unified framework for π and γ processes. He reports good results for the $M_{1+}(\frac{3}{2})$ amplitude.

Among the older models for pion photoproduction we should not ignore the famous Chew, Goldberger, Low, and Nambu[40] dispersion relation approach which assigns an important role to unitarity and analyticity.

Three experiments have been reported[15,41,42] on the recoil-proton polarization P in π^- photoproduction on a neutron, using a deuterium target. Because the neutron
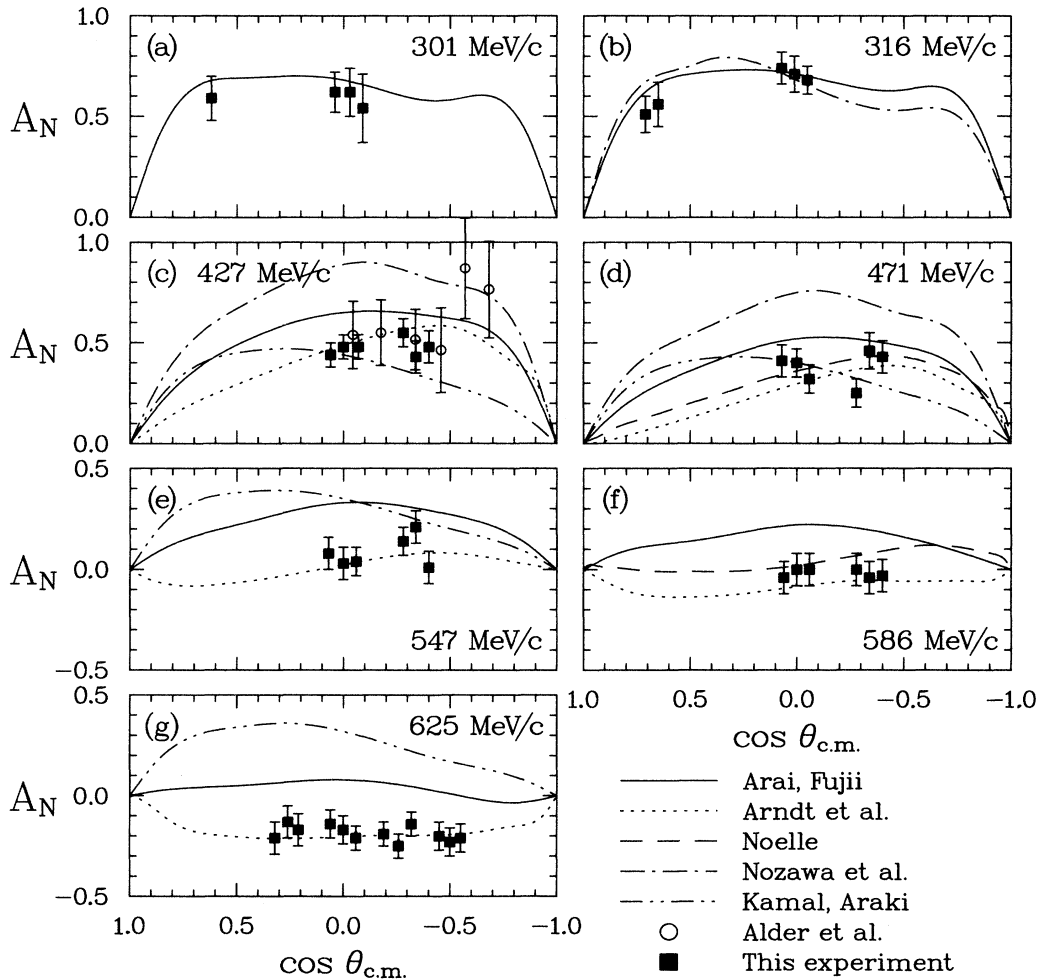
FIG. 5. The left-right asymmetry A_N measured in $\pi^- p \rightarrow \gamma n$ using a transversely polarized target. The solid curves are the predictions from the single-pion photoproduction PWA of Arai and Fujii (Ref. 21), and the dotted curves are from VPI (Ref. 20). (a) Data at $p_\pi = 301$ MeV/c. (b) Data at $p_\pi = 316$ MeV/c. The dot-dashed curve is the quark-model calculation by Nozawa, Blankleider, and Lee (Ref. 38). (c) Data at $p_\pi = 427$ MeV/c. The open circles are the data of Alder et al. (Ref. 11). In addition to the calculation of Nozawa, Blankleider, and Lee, the calculation by Kamal and Araki (Ref. 37) is given by the dot-dot-dashed curve. (d) Data at $p_\pi 471$ MeV/c. The dashed curve is the prediction by Noelle (Ref. 24). (e) Data at $p_\pi = 547$ MeV/c. (f) Data at $p_\pi = 586$ MeV/c. The dashed curve is the prediction by Noelle (Ref. 24) at $p_\pi = 575$ MeV/c. (g) Data at $p_\pi = 625$ MeV/c.

TABLE V. Predictions for the radiative decay amplitudes for $P_{33}(1232)$ and $P_{11}(1440)$ resonances. The helicity amplitudes are given in units of $10^{-3}\,\mathrm{GeV}^{-1/2}$.

$P_{33}(1232)$		$P_{11}(1440)$	
$A_{1/2}$	$A_{3/2}$	$A^n_{1/2}$	Reference
Partial-wave analyses			
-140	-247	$+62$	Noelle[24]
-145 ± 15	-263 ± 26	$+56\pm15$	Crawford-Morton[23]
-147 ± 1	-264 ± 2	$+23\pm9$	Arai-Fujii[21]
		-29 ± 35	Takeda *et al.*[25]
		$+30\pm3$	Fujii *et al.*[26]
-138 ± 4	-259 ± 6	$+37\pm10$	Awaji *et al.*[27]
-141 ± 5	-258 ± 11	$+37\pm19$	Particle Data Group[28]
-133 ± 7	-244 ± 8	$+50\pm19$	VPI(SP89)[20]
Quark models			
-104	-180	$+17$	Copley *et al.*[3]
-108	-187	-18	Feynman *et al.*[4]
-103	-179	$+16$	Koniuk-Isgur[30]
-102	-176		Donoghue *et al.*[31]
-141	-254		Kalbermann-Eisenberg[32]
	-206	$+48$	Bermuth *et al.*[35]

in the deuteron is bound, corrections are needed to account for the effects of Fermi motion, the Pauli exclusion principle in the final state of $\gamma d \to \pi^- pp$, and the strong final-state interactions. In the case of the differential cross-section measurements, a Chew-Low-type extrapolation may be possible. The correct way to do this for recoil-proton polarization remains to be explored.

The earliest experiment on recoil-proton polarization was done by Kenemuth and Stein.[41] They investigated only one point at 90° for E_γ in an interval from 620 to 820 MeV without a measurement of the pion momentum. Beneventano *et al.*[15] employed a single-arm spectrometer for the π^-, but the proton was only measured with limited accuracy. Their data are only at 90° with E_γ in 90-MeV-wide bins between 515 and 714 MeV. The most recent work was done by Takeda *et al.*[42] They used a double-arm spectrometer and obtained results at 60°, 70°, 80°, 90°, and 100° for E_γ between 700 and 1200 MeV in 100-MeV bins. In all three cases the impulse approximation was used and the kinematics of a free neutron target was assumed. No detailed deuterium corrections were applied. The comparison of our A_N results at 90° with P of the inverse reaction is shown in Fig. 6. By time-reversal invariance we have

$$A_N = +P \ .$$

The positive sign is required by the Basel polarization convention. The agreement is qualitative, even with the last and best of the three experiments. This shows the limitations of the impulse approximation in π^- photoproduction on a deuterium target. Until suitable deuterium corrections are available, the REX process should be used for π^- photoproduction.

The 90° excitation spectrum of A_N shown in Fig. 6 indicates that A_N changes sign near $p_\pi = 600$ MeV/c, which coincides with the onset of the Roper resonance. The change in sign is consistent with the M_{1-} multipole becoming more important than M_{1+} in Eq. (1) and with the radiative decay amplitudes of the P_{11} and P_{33} having opposite sign.

FIG. 6. Asymmetry A_N at 90° c.m. obtained in this experiment compared to the recoil-proton polarization P measured in π^- photoproduction using a deuterium target by Kenemuth and Stein (Ref. 41), Beneventano *et al.* (Ref. 15), and Takeda *et al.* (Ref. 42). The solid line is the multipole analysis of Arai and Fujii (Ref. 21), the dashed line by Noelle (Ref. 24), and the dotted curve by VPI (Ref. 20).

V. SUMMARY AND CONCLUSION

We have measured the left-right asymmetry of $\pi^- p \to \gamma n$ using a transversely polarized target from 301 to 625 MeV/c mainly at 90° and 110° c.m., with an accuracy of about ±0.07. Our results support the VPI multipole analysis but disagree somewhat with the Arai-Fujii analysis. Comparing our data to the recoil-proton polar-

ization of the inverse reaction extracted from $\gamma d \rightarrow \pi^- X$ experiments, the difference is typically 20%. The poor agreement casts doubt on the multipole values established from deuterium data used by the Particle Data Group. In the region of $\Delta(1232)$ our data support the chiral-bag-model calculation of Kamal and Araki and the dynamical-model calculation of Nozawa, Blankleider,and Lee, but at higher energies there is substantial disagreement.

ACKNOWLEDGMENTS

*Current address: Cyclotron Institute, Texas A&M University, College Station, TX 77843.

†Current address: Lawrence Livermore National Laboratory, Livermore, CA 94550.

‡Current address: Los Alamos National Laboratory, Los Alamos, NM 87545.

§Current address: Physics Department, University of Bonn, Germany.

[1]R. Wilson, Phys. Rev. 110, 1212 (1958).

[2]R. H. Dalitz, in Proceedings of the 13th International Conference on High Energy Physics, Berkeley, California, 1966 (University of California Press, Berkeley, 1967).

[3]L. A. Copley, G. Karl, and E. Obryk, Nucl. Phys. B13, 303 (1969).

[4]R. P. Feynman, M. Kislinger, and F. Ravndal, Phys. Rev. D 3, 2706 (1971).

[5]N. Isgur, G. Karl, and R. Koniuk, Phys. Rev. D 25, 2394 (1982).

[6]T. Barnes and F. E. Close, Phys. Lett. 116B, 365 (1982).

[7]M. Chanowitz and S. Sharpe, Nucl. Phys. B222, 211 (1983).

[8]T. Barnes and F. E. Close, Phys. Lett. 123B, 89 (1983).

[9]T. Barnes and F. E. Close, Phys. Lett. 128B, 277 (1983).

[10]R. G. Moorhouse, Phys. Rev. Lett. 16, 772 (1966).

[11]J. C. Alder, C. Joseph, J. P. Perroud, M. T. Tran, G. H. Eaton, R. Frosh, H. Hirshmann, S. Mango, J. W. McCulloch, P. Shrager, G. Strassner, P. Truol, P. Weymuth, and P. Wiederkehr, Phys. Rev. D 27, 1040 (1983).

[12]J. Bernstein, G. Feinberg, and T. D. Lee, Phys. Rev. 139, B1650 (1965).

[13]G. J. Kim, J. Arends, W. J. Briscoe, J. Engelage, B. M. K. Nefkens, M. E. Sadler, and H. J. Ziock, Phys. Rev. D 40, 244 (1989).

[14]R. L. Walker, Phys. Rev. 182, 1729 (1969).

[15]M. Beneventano, S. D'Angelo, F. De Notaristefani, P. Monacelli, L. Paoluzi, F. Sebastiani, M. Severi, and B. Stella, Lett. Nuovo Cimento 3, 840 (1970).

[16]G. J. Kim, S. D. Adrian, J. Arends, W. J. Briscoe, A. D. Eichon, J. Engelage, S. Graessle, B. M. K. Nefkens, Y. Ohashi, M. E. Sadler, C. J. Seftor, D. I. Sober, M. Taragin, and H. J. Ziock, Phys. Rev. Lett. 56, 1779 (1986).

[17]G. J. Kim, Ph.D. thesis, University of California at Los Angeles, 1988.

[18]G. J. Kim, J. Arends, W. J. Briscoe, J. Engelage, B. M. K. Nefkens, M. E. Sadler, M. Taragain, and H. J. Ziock, Phys.

Rev. D 41, 733 (1990).

[19]R. Arndt, in Proceedings of the Third International Conference on Pion-Nucleon and Nucleon-Nucleon Physics, Gatchina, U.S.S.R., 1989, edited by I. V. Lopatin and N. C. Morosova (Academy of Sciences of the U.S.S.R., Leningrad, 1989); and (unpublished).

[20]R. Arndt (private communication).

[21]I. Arai and H. Fujii, Nucl. Phys. B194, 251 (1982).

[22]I. M. Barbour, R. L. Crawford, and N. H. Parsons, Nucl. Phys. B141, 253 (1978).

[23]R. L. Crawford and W. T. Morton, Nucl. Phys. B211, 1 (1983).

[24]P. Noelle, Prog. Theor. Phys. 60, 778 (1978); Ph.D. thesis, University of Bonn, Bonn Report Bonn-IR-75-20, 1977 (unpublished).

[25]H. Takeda et al., Nucl. Phys. B168, 17 (1980).

[26]K. Fujii et al., Nucl. Phys. B187, 53 (1981).

[27]N. Awaji et al., Nucl. Phys. B197, 365 (1982).

[28]Particle Data Group, G. P. Yost et al., Phys. Lett. B 204, 366 (1988).

[29]D. Faiman and A. W. Hendry, Phys. Rev. 180, 1572 (1969).

[30]N. Isgur and G. Karl, Phys. Rev. D 18, 4187 (1978); 19, 2653 (1979); R. Koniuk and N. Isgur, ibid. 21, 1868 (1980).

[31]J. F. Donoghue, E. Golowich, and B. Holstein, Phys. Rev. D 12, 2875 (1975).

[32]G. Kalbermann and J. M. Eisenberg, Phys. Rev. D 28, 71 (1983).

[33]M. Araki and A. M. Kamal, Phys. Rev. D 29, 1345 (1983).

[34]M. Weyrauch, Phys. Rev. D 35, 1574 (1987).

[35]K. Bermuth, D. Drechsel, L. Tiator, and J. Seaborn, Phys. Rev. D 37, 89 (1988).

[36]M. Araki and I. R. Afnan, Phys. Rev. C 36, 250 (1987).

[37]A. N. Kamal and M. Araki, Phys. Rev. C 38, 1335 (1988).

[38]S. Nozawa, B. Blankleider, and T. S. H. Lee, Nucl. Phys. A513, 459 (1990); and (unpublished).

[39]S. N. Yang, J. Phys. G 11, L205 (1985).

[40]G. F. Chew, M. L. Goldberger, F. E. Low, and Y. Nambu, Phys. Rev. 106, 1345 (1957).

[41]J. R. Kenemuth and P. C. Stein, Phys. Rev. 129, 2259 (1963).

[42]H. Takeda, I. Arai, T. Fujii, H. Ikeda, H. Iwasaki, N. Kajiura, T. Kamae, S. Kawabata, K. Ogawa, T. Sumiyoshi, H. Fujii, S. Homma, M. Kanazawa, and N. Yamashita, Nucl. Phys. B168, 17 (1980).